MODE I FRACTURE CHARACTERIZATION OF WOOD USING THE SEN-TPB TEST

N. Dourado[1,*], M.F.S.F. de Moura[2], J.J.L. Morais[1]

[1]CITAB/UTAD, Departamento de Engenharias, Quinta de Prados, 5001-801 Vila Real, Portugal
[2]Faculdade de Engenharia da Universidade do Porto, Departamento de Engenharia Mecânica, Rua Dr. Roberto Frias, 4200-465 Porto, Portugal
* E-mail: nunodou@gmail.com

ABSTRACT

The single-edge-notched beam loaded in three-point-bending has been numerically analyzed to validate its adequacy to characterize wood fracture under pure mode I loading. This specimen geometry has been chosen since it is particularly useful to perform tests in those fracture systems impossible to be tested with the double cantilever beam (DCB). The study revealed several aspects avoiding the direct measurement of fracture toughness in wood due to confinement of the fracture process zone (FPZ) under loading. This has been confirmed analyzing stress profiles of different specimen sizes, differently affected by compression due to bending.

KEYWORDS: Wood, cohesive modeling, stress relief zone, mode I.

1. INTRODUCTION

Wood is usually regarded as a continuum, homogeneous and orthotropic material exhibiting three anatomic directions: longitudinal (L), radial (R) and tangential (T), (Fig. 1a). Consequently, six independent crack propagation systems are defined: TL, RL, LR, TR, RT and LT (Fig. 1b). In these fracture systems the first letter indicates the direction perpendicular to the crack plane, while the second defines the direction of crack propagation. Among the most frequent crack propagation systems in timber structures one can point the TL and RL. Due to test simplicity and applicability of beam theory the double cantilever beam (DCB) is particularly adequate to evaluate fracture energy [1, 2].

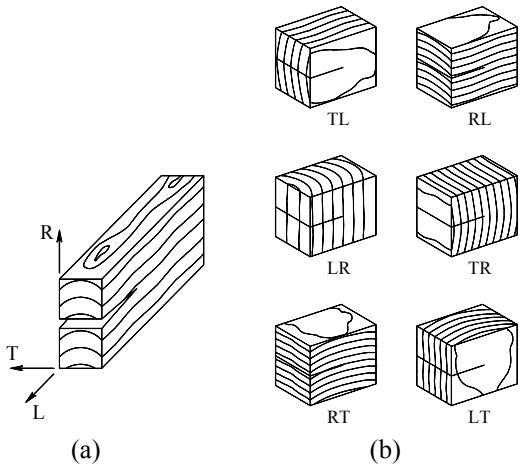

Figure 1. Anatomic axis of wood: (a) Longitudinal (L), Radial (R) and Tangential (T), (b) Wood fracture systems.

Nevertheless, the DCB is barely suitable to perform fracture tests in RL and TL propagation systems, as crack in these orientations propagate along wood fibre directions. In regards to the remaining ones (i.e., TR and RT) the DCB is not suitable, being affected by a non-negligible stick-slip effect. As a result, crack in these cases deviates from the mid-plane, inducing mixed-mode loading in place of the pretended pure mode I. Besides due to the curvature of wood annual rings it turns unfeasible to manufacture DCB specimens for fracture systems TR and RT.

Another aspect as to due with the fact that once located satisfactorily distant from the log pith, wood is frequently treated as a cylindrically orthotropic material, as the curvature of annual rings is less obvious. Furthermore, one should note that wood fracture tests might be performed in specimens free from knots or other material defects (e.g., resin pockets), which is exceptionally difficult to achieve with the DCB, due to the required length. This issue is particularly important when a size effect study is envisaged. In such a case, other geometries exist to induce mode I fracture in wood such as the compact tension test (CT) [3], the wedge split test (WS) [4] and the single-edge-notched beam loaded in three-point-bending (SEN-TPB) test [5, 6, 7] (Fig. 2). The CT has firstly been applied by Boström [3] to perform the theoretical estimate of initiation and growth of fracture process zone (FPZ) in wood, thus providing the assessment of the corresponding value of the critical stress intensity factor. Boström observed that the load-displacement response is susceptible to wood elastic modulus perpendicular to grain, as well as the tensile strength,

fracture energy and specimen size. In regards to the WS test, first proposed by Stanzl-Tschegg et al. [4] to characterize wood under fracture, a pair of load transmission pieces is put in contact with wood while a slight wedge (angle of 5-10°) is displaced along the notch direction. According to the authors, the energy losses are considerably reduced with this loading apparatus, since friction is minimized by means of roles used to transmit the pair of loads from the wedge to the wood specimen. Stable crack initiation and growth is thus achieved as the applied load induced by the wedge is split in two forces towards the wood notch surface.

It is recognizable that the SEN-TPB is considerably easier to perform than the WS test, since it does not necessitate the use of special devices (wedges and rolling devices). This is particularly useful when size effect studies are envisaged, as it requires undergoing fracture tests in different specimen sizes. Gustafsson [6] observed that consistent wood fracture parameters are obtained using a set of specimens (SEN-TPB) with small size. This observation is relevant, as it turns easier to select wood test volumes free from knots and defects. First reported studies in the literature involving the SEN-TPB to evaluate fracture energy in wood have been performed by Daudeville [7] for the fracture systems RL and TL.

A recent work performed by Dourado et al. [5] using cohesive models on the SEN-TPB in two different wood species (Pinus pinaster Ait. and Picea abies L.) proved the efficacy of this test in mode I fracture characterization of wood. The authors observed the existence of an interaction between the cohesive zone (CZ) ahead of the crack tip with the specimen boundaries, which was considered to be a critical aspect on the definition of the specimen size. Since the interaction of the CZ with the specimen boundaries increases artificially the fracture energy, then the right choice of the specimen size in this test is a fundamental aspect.

The goal of this work is to develop an appropriate data reduction method to be applied on the SEN-TPB test for wood fracture characterization under pure mode I loading. The proposed method is based on beam theory and crack equivalent concept overcoming the difficulty of crack measurement during its growth. It was verified that a triangular stress relief region exists in the vicinity of the crack tip. The theoretical application o f the proposed methodology includes this important issue. The model was validated numerically by means of a pure mode I damage model.

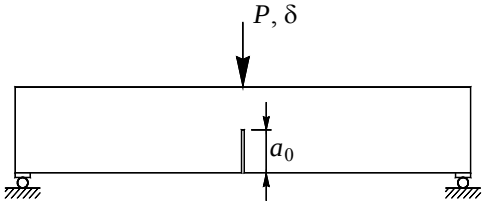

Figure 2 – Representation of the SEN-TPB test.

2. NUMERICAL ANALYSIS

The SEN-TPB specimen is constituted by a central region oriented according to the chosen wood fracture system (i.e., TL), bonded to a pair of arms (Fig. 3) aligned with wood fiber direction (i.e., L) to assure high bending stiffness. Though recognizing that the aim of this test is to be applied in planes where the DCB does not perform well (TR and RT), this system (i.e., TL) was chosen to validate the proposed data reduction method as it was previously characterized in a preceding work [5]. Hence, a finite element analysis (FEA) using plane strain elements and a cohesive damage model [8] was performed considering H=70 (b=20 mm). Due to the specimen symmetry only the half specimen was simulated. The finite element (FE) mesh has been implemented to provide a ligament length uniformly divided in every 0.5 mm. Figure 4 illustrates the sketch of the FE mesh presenting 837 solid elements (8-node quadrilateral and 6-node triangular), with 64 cohesive elements (6-node). Norway spruce (*Picea abies* L.) material properties (Table 1) were used in the numerical simulations.

Figure 5 illustrates the bilinear damage model used to simulate damage initiation and growth, presenting the set of cohesive properties shown in Table 2. Previous studies [4, 9] revealed the adequacy of this damage model to simulate damage initiation and growth in wood since it allows replicating two fracture phenomena observed in the course of the loading process: micro-cracking (first branch of the softening law) and fibre-bridging (second one). More details of the cohesive damage law can be found in references [1, 5]. In order to avoid unstable crack propagation, mode I loading was induced by means of displacement control, using very small loading increments. Since the aim of this study is to determine the *Resistance*-curve (*R*-curve) in wood, the load-displacement curve (Fig. 6) was recorded. To conclude, the performance of the method will be evaluated by comparing the G_{Ic} obtained from the plateau of the *R*-curve with the inputted value (G_{Ic}(inp)) through the cohesive damage model.

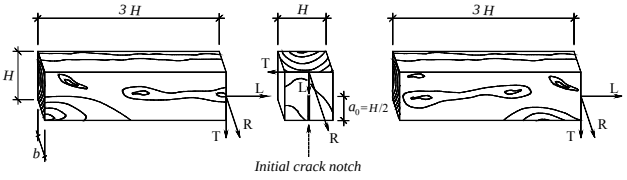

Figure 3 – Bonding setup before bonding.

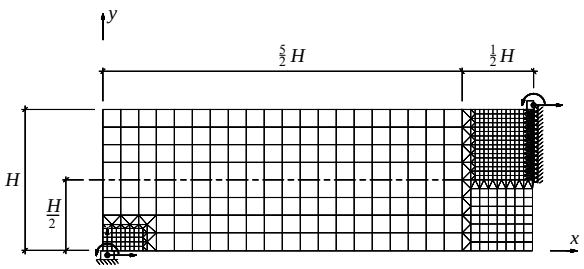

Figure 4 – Mesh sketch used in the simulations.

Table 1 – Elastic properties of *Picea abeas* L. [10]

E_L (MPa)	E_R (MPa)	E_T (MPa)	ν_{LT}	ν_{LR}	ν_{TR}
9 900	730	334	0.435	0.430	0.249

G_{TL} (MPa)	G_{RT} (MPa)	G_{RL} (MPa)
610	22	500

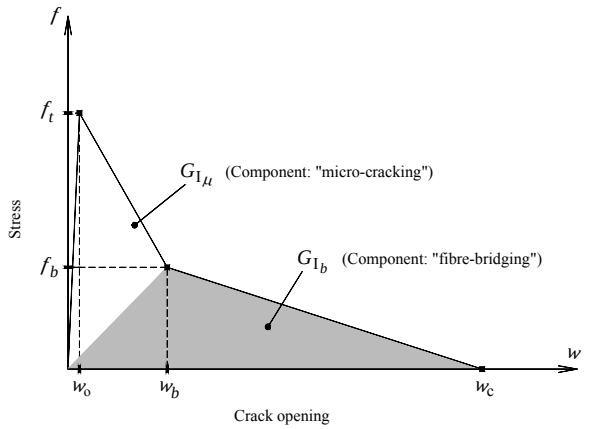

Figure 5 – Bilinear cohesive damage model [8].

Table 2 – Cohesive properties of *Picea abeas* L. [5]

f_t (MPa)	f_b (MPa)	w_b (mm)	G_f (N/mm)
1.66	0.30	0.09	0.145

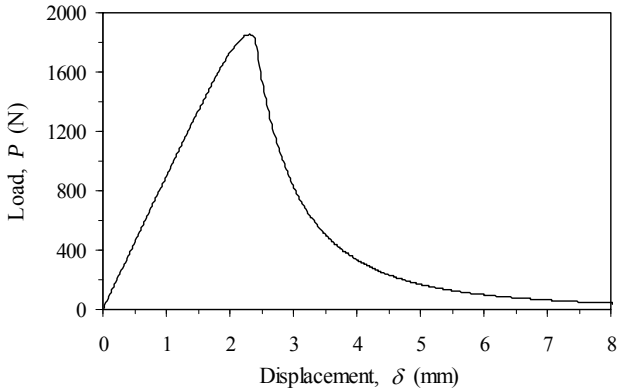

Figure 6 – P-δ curve issued from the FE simulation.

3. DATA REDUCTION SCHEME

Classical data reduction schemes frequently applied to measure the fracture energy are not adequate for the SEN-TPB specimen. On the other way, compliance calibration methods necessitate the crack monitoring during its growth which is not feasible in this test. In fact, crack grows rapidly and the presence of fibre bridging hinders a clear identification of its tip. Moreover, the size of the FPZ developed ahead of the crack tip can be affected in some specimen sizes by the normal compressive stresses due to bending, above the specimen neutral axis [5]. This spurious effect modifies the conditions of self-similar crack growth, thus affecting the measured energy. In order to overcome these disadvantages and to identify adequate specimen sizes, a new data reduction scheme based on beam theory and crack equivalent concept was used.

One of the aspects that lead to difficulties on the direct application of beam theory concepts is associated to the presence of the crack development which modifies the bending stress profile in its vicinity. Kienzler and Herrmann [11] suggested that in the SEN-TPB an approximately triangular stress relief region (SRR) can be considered, as represented in Fig. 7. In the interior of the SRR the normal stresses induced by bending drop approximately to zero and this must be taken into account in the analysis. According to the notation used to define the specimen geometry illustrated in Fig. 7, the SRR develops in the range: $L_2 \le x \le L$. This means that for $x < L_2$ stress profiles are well previewed by beam theory. Therefore, the strain energy due to bending can be written as

$$U = 2\left[\int_0^{L_2} \frac{M_f^2}{2E_L I}dx + \int_{L_2}^{L_1} \frac{M_f^2}{2E_L I_{sr}}dx + \int_{L_1}^{L} \frac{M_f^2}{2E_T I_{sr}}dx\right] \quad (1)$$

with M_f stands for the bending moment ($M_f = Px/2$) and E_L and E_T the Young's modulus on the longitudinal and transverse direction, respectively (Fig. 3). Parameters I and I_{sr} represent the second moment of area of the entire section (height H) and the effective section within the SRR (height $h(x)$), respectively (Fig. 7). These quantities can be written as follows,

$$I = \frac{bH^3}{12}\ ;\ I_{sr} = \frac{b\left(h(x)\right)^3}{12} \quad (2)$$

being b the specimen width (Fig. 3) and

$$h(x) = H + \frac{a}{L - L_2}\left(L_2 - x\right) \quad (3)$$

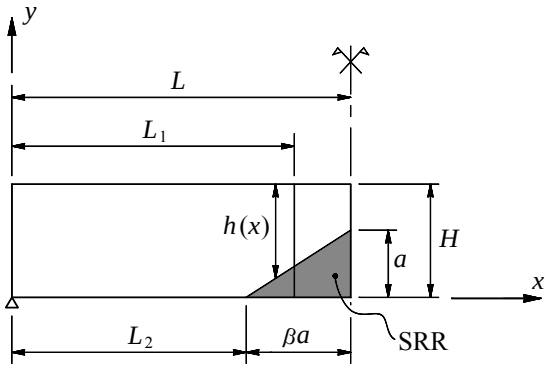

Figure 7. Notation used for the geometry definition.

a is the crack length (Fig. 7). Combining equations (2) and (3) in equation (1), and applying the Castigliano theorem

$$\delta = \frac{\partial U}{\partial P} \tag{4}$$

the applied displacement value δ (Fig. 2) is obtained. The specimen compliance ($C = \delta/P$) can be written as follows,

$$C = \frac{2L_2^3}{E_L b H^3} + \frac{6(L-L_2)}{ba}\left\{\frac{1}{E_L}\left[\frac{L_1^2}{2(h(L_1))^2} - \frac{L_2^2}{2H^2} + \frac{L-L_2}{a}\left(\frac{L_2}{H} - \frac{L_1}{h(L_1)}\right) + \left(\frac{L-L_2}{a}\right)^2 \ln\frac{H}{h(L_1)}\right] + \frac{1}{E_T}\left[\frac{L^2}{2(H-a)^2} - \frac{L_1^2}{2(h(L_1))^2} + \frac{L-L_2}{a}\left(\frac{L_1}{h(L_1)} - \frac{L}{H-a}\right) + \left(\frac{L-L_2}{a}\right)^2 \ln\frac{h(L_1)}{H-a}\right]\right\} \tag{5}$$

with $h(L_1)$ being obtained from equation (3), considering $x=L_1$. Equation (5) establishes the relation $C=f(a)$ accounting for a triangular SRR (Fig. 7). Nevertheless, there are additional issues that can affect the accuracy of equation (5) before damage onset. For instance, shear effects were not taken into account. Its effect cannot be considered as non negligible, in particular when higher specimens are analysed. On the other hand, due to stress concentrations in the vicinity of the crack tip the characteristic stress profile induced by bending is altered. At last, it is known that wood presents important scatter in its elastic properties [12], which means that the elastic modulus E_T (Fig. 3) can vary considerably from specimen to specimen. Therefore, with the aim of overcoming these inaccuracies, a corrected value of the flexural modulus (E_{Tf}) has been defined in the place of the nominal one. This quantity (E_{Tf}) can easily be computed for each specimen from equation (5), taking into consideration the initial values of compliance C_0 and crack length a_0, which must be accurately measured. In regards to the elastic modulus E_T no correction has been performed since the specimen lateral arms to be used in the experiments are to be reutilised (usually the same arms are used for all tests performed for a given specimen size), being previously characterised. Furthermore, Morel et al., 2005 [13] have demonstrated that the contribution of E_T to the specimen compliance is negligible for the SEN-TPB test (Fig. 3).

As previously referred crack length cannot be accurately measured in wood fracture during its growth. However, an equivalent value of the crack length (a_e) can be established as a function of the current compliance using equation (5). As no analytical solution is possible to provide, the bisection method has been used to determine the value of a_e from equation (5) for each point of the P-δ curve. Then, the strain energy release rate is obtained using the Irwin-Kies equation

$$G_I = \frac{P^2}{2b}\frac{dC}{da} \tag{6}$$

Thus, considering a_e in equation (5), instead of a, yields

$$G_I = \frac{3P^2(L-L_2)}{b^2}\left\{\frac{1}{E_L}\left[\frac{L_2^2}{2H^2a_e^2} - \frac{L_1^2(H+3ka_e)}{2a_e^2(H+ka_e)^3} + (L-L_2)\left(\frac{L_1(2H+3ka_e)}{a_e^3(H+ka_e)^2} - \frac{2L_2}{Ha_e^3}\right) - \frac{(L-L_2)^2}{a_e^3}\left(\frac{3}{a_e}\ln\frac{H}{H+ka_e} + \frac{k}{H+ka_e}\right)\right] + \frac{1}{E_{Tf}}\left[\frac{L^2(3a_e-H)}{2a_e^2(H-a_e)^3} + \frac{L_1^2(H+3ka_e)}{2a_e^2(H+ka_e)^3} - (L-L_2)\left(\frac{L_1(2H+3ka_e)}{a_e^2(H+ka_e)^2} + \frac{L(3a_e-2H)}{a_e^3(H-a_e)^2}\right) + \frac{(L-L_2)^2}{a_e^3}\left(\frac{H(1+k)}{(H-a_e)(H+ka_e)} - \frac{3}{a_e}\ln\frac{H+ka_e}{H-a_e}\right)\right]\right\} \tag{7}$$

with $k = (L_2-L_1)/(L-L_2)$. Therefore, the R-curve is estimated without performing the crack length monitoring during its propagation. According to this procedure the unique parameter that has be determined is the length L_2, which is used to define the SRR (Fig. 7).

4. RESULTS

In the numerical study six homothetic specimen sizes were analysed ($17.5 \le H \le 560$ mm). The goal was to obtain the minimum dimension allowing the appropriate replication of the inputted value of G_{Ic} (*i.e.*, G_{Ic}(inp)), in the plateau of the R-curve. Besides, the estimation of the length L_2 was also necessary. In the following discussion the horizontal cathetus of the triangular SRR was assumed to be a linear function of the crack length, *i.e.*, $L - L_2 = \beta a$, being β a constant to be defined. In fact, when the crack grows the resistant ligament extent (H-a) diminishes (Fig. 7), thus decreasing L_2 and increasing the SRR.

Figure 8 presents the R-curve obtained for the specimen size H=70 mm. The value of β originating a plateau approximately equal to unity is presented. It was verified that for $H \ge 70$ mm a constant value of β is obtained. Contrarily, for $H < 70$ mm different values for β are obtained, and the plateau practically does not exist (H = 17.5 mm) or is quite short (H = 35 mm). It can be concluded that these dimensions are not adequate for fracture characterization of this material with this test. In fact, in these smaller specimens the normal compressive stresses induced by bending above the specimen neutral axis hinder a self-similar crack growth from a certain point.

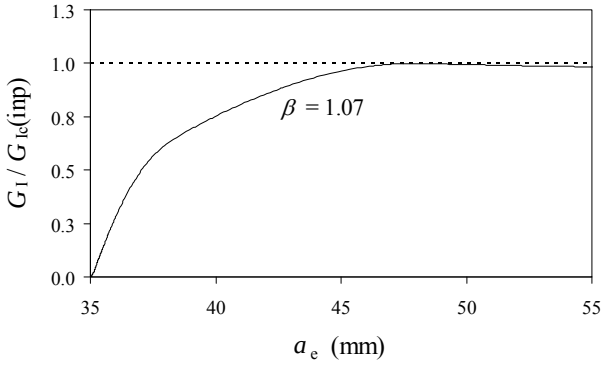

Figure 8 – R-curve.

5. CONCLUSIONS

A new data reduction scheme based on equivalent crack concept, beam theory and specimen compliance was developed for the SEN-TPB test applied to fracture characterization of wood under mode I loading. The method accounts for a triangular stress relief region in the vicinity of the crack, which was verified to be a fundamental issue in order to replicate accurately the inputted toughness. The size of the stress relief region is dictated by an independent parameter which was verified to converge for a constant value for higher specimen sizes. The obtained values points to an approximately isosceles triangle which is in agreement with the conclusions of Kienzler and Herrmann [11]. The present study also revealed that self-similar crack growth, which reflects on an undoubtedly plateau on the *R*-curve, only occurs for specimens with $H \geq 70$ mm. It can be concluded that the proposed methodology is a essential contribution to the use of the SEN-TPB test, on wood fracture characterization under mode I loading.

6. REFERENCES

[1] de Moura MFSF, Morais J, Dourado N. A new data reduction scheme for mode I wood fracture characterization using the double cantilever beam test. Eng Fract Mech 2008;75:3852-65

[2] Yoshihara H, Kawamura T. Mode I fracture toughness estimation of wood by DCB test. Compos: Part A 2006;37: 2105–13.

[3] Boström L. The stress-displacement relation of wood perpendicular to the grain. Wood Sci Technol 1994;28:319-27.

[4] Stanzl-Tschegg SE, Tan DM, Tschegg EK. New splitting method for wood fracture characterization. Wood Sci Technol 1995;29:31–50.

[5] Dourado N, Morel S, de Moura MFSF, Valentin G, Morais J. Comparison of fracture properties of two wood species through cohesive crack simulations. Compos: Part A 2008;39 415–27.

[6] Gustafsson PJ (1988). A study of strength of notched beams. Paper 21-10-1. In: Proceedings of CIB-W18A Meeting, Parksville, Canada.

[7] Daudeville L. Fracture in spruce: experiment and numerical analysis by linear and non linear fracture mechanics, Holz als Roh und Werkstoff 1999;57: 425-32.

[8] Petersson PE. Crack growth and development of fracture zone in plain concrete and similar materials. Report No. TVBM-1006, Division of Building Materials, Lund Institute of Technology, Lund, Sweden; 1981.

[9] Dourado N. *R*-Curve behaviour and size effect of a quasibrittle material: Wood. PhD Thesis. Université de Bordeaux I (FR) in co-tutorship with University of Trás-os-Montes and Alto Douro (PT). 2008.

[10] Guitard D. Mécanique du matériau bois et composites. Cepadues-Editions. ISBN 2.85428.152.7:108-23¸1987.

[11] Kienzler R and Herrmann G. An elementary theory of defective beams. Acta Mech, 1986;62:37-46.

[12] de Moura MFSF, Silva MAL, Morais J, de Morais AB, Lousada JJL. Data reduction scheme for measuring G_{IIc} of wood in End-Notched Flexure (ENF) tests. Holzforschung 2009;63:99-106.

[13] Morel S, Dourado N, Valentin G, Morais J. Wood: a quasibrittle material - *R*-curve behavior and peak load evaluation. Int J Fracture 2005;131:385–400.